

DETERMINATION OF THE EMITTER SATURATION CURRENT DENSITY OF SILICON SOLAR CELLS USING PHOTOLUMINESCENCE AND QUANTUM EFFICIENCY ANALYSIS

David Hinken, Karsten Bothe, Klaus Ramspeck, Sandra Herlufsen and Rolf Brendel
 Institut für Solarenergieforschung Hameln (ISFH)
 Am Ohrberg 1, D-31860 Emmerthal, Germany

ABSTRACT: We determine the emitter saturation current density J_{0e} of silicon solar cells using a combined approach of photoluminescence (PL) and quantum efficiency (QE) measurements. We prove that the ratio of two PL measurements obtained under open circuit and short circuit conditions yields the saturation current density J_0 . We obtain the saturation current density contribution of the base J_{0b} from quantum efficiency measurements. The difference between the total saturation current density J_0 and J_{0b} yields the emitter saturation current density. This analysis is applied to both, a high-efficiency solar cell as well as to a standard industrial solar cell. The benefit of using photoluminescence is a possible spatially resolved application if combining camera-based PL measurements with mappings of the effective diffusion length.

Keywords: Luminescence, Solar Cell, Characterisation

1 INTRODUCTION

The efficiency of crystalline silicon solar cells is limited by resistive and recombination losses. In this work we concentrate on the recombination losses which include recombination within the bulk of the solar cell, at the surfaces and within the emitter. Bulk and rear surface recombination are determined using quantum efficiency analysis [1]. Recombination in the volume of the emitter and at the front surface is lumped into the emitter saturation current density J_{0e} . For solar cells with effective minority carrier diffusion lengths larger than twice its cell thickness J_{0e} becomes the efficiency-limiting parameter.

The total saturation current density J_0 is the sum of the base saturation current density J_{0b} and the emitter saturation current density J_{0e} if parasitic shunt currents are negligibly small. Quantum efficiency (QE) analysis yields the effective diffusion length L_{eff} and thus the base saturation current density J_{0b} .

For the determination of J_0 we measure the optically stimulated luminescence emission under open circuit and short circuit conditions. It was shown in Ref. 2 that the ratio of these two luminescence emissions is a measure of the effective diffusion length L_{eff} and the effective emitter recombination velocity S_{em} . We extend the approach of Ref. 2 and show that the PL ratio directly gives the total saturation current density J_0 .

The benefit of using photoluminescence is a possible spatially resolved application. Combining camera-based photoluminescence measurements [3] with mappings of the effective diffusion length, as for example obtained by spectrally resolved light beam induced current (SR-LBIC) [4], determines mappings of the emitter saturation current density.

In this work, we evaluate the proposed approach. We prove experimentally that the PL ratio of the open circuit and short circuit luminescence emission gives the total saturation current density. In combination with quantum efficiency analysis we obtain the emitter saturation current density for a high-efficiency solar cell as well as for a standard industrial solar cell and discuss the results.

2 THEORY

The emitter saturation current density J_{0e} is a parameter which lumps carrier losses in the volume of the emitter and at the front surface into one single value. The impact of J_{0e} on the carrier distribution within the solar cell is described using an effective emitter surface recombination velocity S_{em} . The emitter is thus reduced to an ideal thin layer with S_{em} acting as a sink at the edge of the space charge region just within the base. S_{em} follows from J_{0e} by [5, 6]

$$J_{0e} = \frac{qn_i^2}{N_A} \cdot S_{em} \quad (1)$$

if carrier losses within the space charge region are small. Here, q is the elementary charge and n_i the intrinsic carrier concentration.

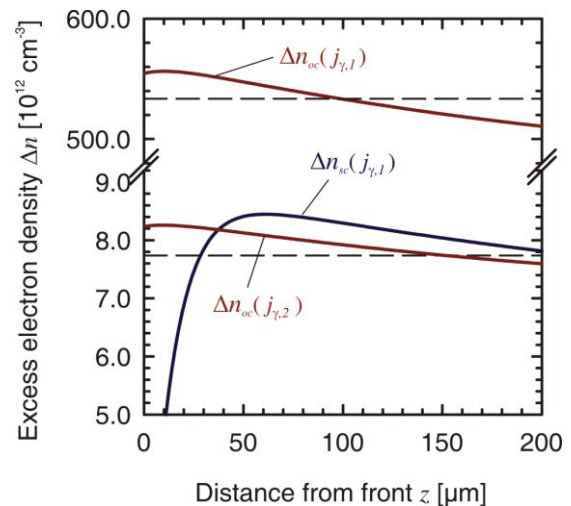


Figure 1: Excess electron densities $\Delta n(z)$ within the base of a solar cell for PL-oc and PL-sc condition under two different illumination intensities $j_{\gamma,1}$ and $j_{\gamma,2}$. The dashed lines indicate the average carrier densities. The parameters used for this simulation are given in Tab. 1.

Recombinations within the bulk of the solar cell and at the rear surface are described using the bulk diffusion length L_b and the rear surface recombination velocity S_r . These two quantities determine the effective diffusion length L_{eff} [1]. L_{eff} again scales with N_A to the bulk saturation current density

$$J_{0b} = \frac{qn_i^2}{N_A} \cdot \frac{D}{L_{eff}}. \quad (2)$$

Here, D is the diffusivity of the charge carriers. The total saturation current density

$$J_0 = J_{0b} + J_{0e} \quad (3)$$

follows as a sum of the base and the emitter saturation current density if currents due to shunts are negligibly small. J_0 is a measure for all carrier losses within the solar cell base and is, in general, dependent on the particular working point of the solar cell. Equation (3) allows for a determination of J_{0e} if J_{0b} and J_0 are known. Using quantum efficiency analysis, J_{0b} is obtained conveniently.

As shown in Ref. 2 the ratio

$$R = \frac{\Phi_{oc}}{j_{\gamma}^{oc}} \cdot \frac{j_{\gamma}^{sc}}{\Phi_{sc}} \quad (4)$$

of the measured photoluminescence emission under open circuit (Φ_{oc}) and short circuit conditions (Φ_{sc}) is

$$\frac{1}{RL_{\alpha}} \cong \frac{1}{L_{eff}} + \frac{S_{em}}{D}. \quad (5)$$

Here, j_{γ}^{oc} and j_{γ}^{sc} are the illumination intensities for open circuit and short circuit conditions and L_{α} is the absorption length in silicon of the monochromatic illumination. Current losses at shunts are assumed to be negligible small.

In this work, we show that the photoluminescence ratio R directly gives the total saturation current density. Multiplying Eq. (5) with Dqn_i^2/N_A gives

$$\frac{D}{RL_{\alpha}} \cdot \frac{qn_i^2}{N_A} \cong J_{0b} + J_{0e} \quad (6)$$

and thus with Eq. (3) the total saturation current density J_0 . If strong shunt resistances or defect-related recombination in the space charge region are present, the determined J_{0e} is increased by a value accounting for these carrier losses. To deal with such solar cells, measurements can be carried out at a working point where the first diode is the dominant recombination path. Another option is to measure the PL ratio at different working points and apply a regression function to obtain the saturation current density of the first diode. The application of such a regression function is well known for I_{sc} - V_{oc} measurements.

Table I: Solar cell parameters for the simulated carrier distributions of Fig. 1.

parameters	
wafer	200 μ m thick, <i>p</i> -type, 1.47 Ω cm
front	$S_f = 35825$ cm/s, <i>n</i> -type emitter, $J_{0e} = 300$ fA/cm ² , $S_{em} = 201$ cm/s
rear	$S_r = 100$ cm/s
volume	$L_b = 800$ μ m, no injection dependence, $D = 28.6$ cm ² /s, $L_{eff} = 1629$ μ m, $L_c = 190$ μ m, $J_{0b} = 262$ fA/cm ²
optics	no exterior front reflection, all internal reflections 100%
illumination	50 and 0.74 mW/cm ² , 808nm

3 SIMULATIONS

We firstly demonstrate the determination of the emitter saturation current density with photoluminescence by simulating PL-oc and PL-sc carrier distributions using the numerical device simulator PC1D [7]. Table 1 lists all relevant parameters used for this simulation. Since carrier losses in the volume of the emitter cannot be described by a specific parameter the emitter is reduced to an ideal thin layer. This allows to directly calculate J_{0e} from the front surface recombination velocity S_f using Eq. (1). Note the difference between S_f and S_{em} . S_f describes the surface recombination velocity at the actual physical front surface while S_{em} is an effective surface recombination that accounts for both, the recombination within the volume of the emitter and the recombination at the actual physical surface.

The carrier distributions for two illumination intensities $j_{\gamma,1}$ and $j_{\gamma,2}$ are shown in Fig. 1 as solid lines. A slight bending of Δn_{oc} for $z \rightarrow 0$ indicates the impact of the emitter saturation current density. The dashed lines in Fig. 1 represent the average carrier densities n_{av} which determine the luminescence emission. n_{av}^{oc} has a value of 533.5×10^{12} cm² and n_{av}^{sc} of 7.73×10^{12} cm².

We demonstrate with the average carrier densities that the PL ratio directly yields the total saturation current density: Inserting $RL_{\alpha} = 827$ μ m in Eq. (6) gives $J_{0,PL} = 554$ fA/cm². J_0 can also be calculated analytically from S_{em} and L_{eff} and we obtain $J_0 = 562$ fA/cm². This value is in good agreement with the result obtained from the PL measurement. Note that RL_{α} can be interpreted as an effective diffusion length describing all recombination properties (front, bulk, rear) of the solar cell.

In this example, $J_{0,PL}$ slightly underestimates the real saturation current density. Simulations show that $J_{0,PL} < J_0$ holds for all cases but that the deviation is small. For realistic parameters ($L_{\alpha} < 12$ μ m, $L_{eff} > 200$ μ m, $J_{0e} < 1000$ fA/cm², $N_A < 2 \times 10^{16}$ cm²) the deviation of $J_{0,PL}$ is always smaller than 10%.

Finally, we subtract the base contribution J_{0b} from J_0 to determine the emitter saturation current density J_{0e} . A value of $L_{eff} = 1629$ μ m yields $J_{0b} = 262$ fA/cm² and we calculate the emitter saturation current density $J_{0e} = 554 - 262$ fA/cm² = 292 fA/cm². This value corresponds well to the real emitter saturation current density fed into the simulation (300 fA/cm²). In the experimental approach, L_{eff} is obtained by quantum efficiency analysis.

4 INJECTION DEPENDENCES

In order to ensure the same injection conditions for PL-oc and PL-sc measurements, we reduce the illumination intensity j_γ for the PL-oc measurement. Since luminescence measurements directly represent the carrier densities [2] the measured PL-oc luminescence emission at j_γ^{oc} has to equal the PL-sc luminescence emission at j_γ^{sc} . For the PL-Ratio R , the different illumination intensities have to be considered as indicated in Eq. (4).

Figure 1 illustrates this procedure. $j_{\gamma,1}$ is reduced to a lower intensity $j_{\gamma,2}$ until the luminescence emission of $\Delta n_{oc}(j_{\gamma,2})$ equals the luminescence emission of the short circuit carrier distribution $\Delta n_{sc}(j_{\gamma,1})$. This results in the same average carrier densities. Moreover, for all $z > 30 \mu\text{m}$ even the depth-dependent carrier distributions $\Delta n_{oc}(j_{\gamma,2})$ and $\Delta n_{sc}(j_{\gamma,1})$ are at nearly the same carrier density for both conditions.

The corresponding operation point of the emitter saturation follows from $\Delta n_{oc}(z)|_{z=0}$. In the simulation this value corresponds to 531 mV. In general, this operation point is quite freely selectable. For solar cell characterisation, the most relevant operation point is the maximum power point.

For the quantum efficiency analysis the injection level is usually determined by the extracted short circuit current density j_{sc}^{QE} . For absolute quantum efficiency measurements this current has to equal the extracted short circuit current j_{sc}^{PL} to maintain equal carrier densities. However, bias light assisted QE measurements determine the differential quantum efficiency [8]. Our approach is to measure the differential EQE bias ramp at a certain wavelength (1000 nm). By integrating these differential EQE-values the corresponding injection level of the absolute measurement follows [9].

5 MEASUREMENTS

We demonstrate the applicability of the presented method by using a quantum efficiency and a photoluminescence setup. The technical details of the quantum efficiency setup are published in Ref. 9 and of the photoluminescence setup in Ref. 2.

5.1 PL ratio vs saturation current densities

We first focus on the experimental demonstration that the PL ratio yields the total saturation current density J_0 . For various silicon solar cells we measure the luminescence emission under open-circuit and short-circuit conditions (PL-oc and PL-sc). The illumination intensity is adjusted for the PL-oc measurement to maintain same carrier densities within the bulk. Using Eq. (4) and Eq. (6) the total saturation current densities follows from the PL ratio. The base dopant density N_A is determined using capacitance voltage (CV) measurements [11].

During the PL measurements the corresponding open-circuit voltage V_{oc} (for PL-oc) and the extracted current J_{sc} (for PL-sc) are determined. As a comparison to the value determined from PL, the total saturation current density

$$J_{0,IV} = \frac{j_\gamma^{oc}}{j_\gamma^{sc}} \cdot \frac{J_{sc}}{\exp(V_{oc}/V_T)} \quad (7)$$

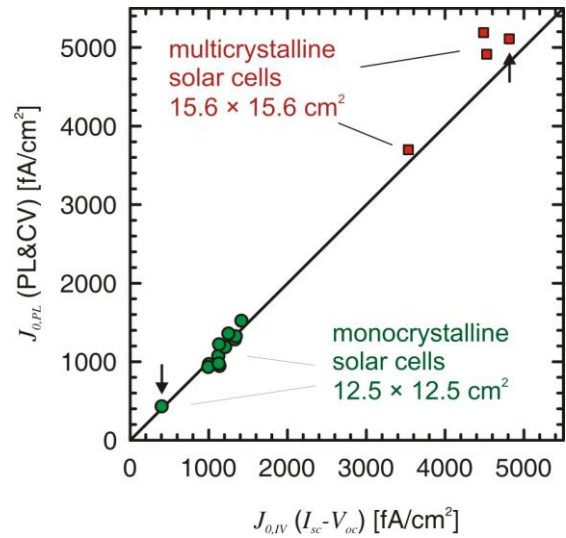


Figure 2: Total saturation current densities of various textured silicon solar cells obtained from photoluminescence (axis of ordinates) and I_{sc} - V_{oc} measurements (axis of abscissae).

then follows directly from the two quantities J_{sc} and V_{oc} and the thermal voltage V_T .

The result of this comparison is shown in Fig. 2. For a wide range of saturation current densities (from 430 to 5000 fA/cm²) a good quantitative agreement is achieved. Figure 2 also demonstrates that I_{sc} - V_{oc} measurements and our PL-based measurement technique obtain identical results.

5.2 Extraction of the emitter saturation current density

In order to demonstrate the combined approach experimentally we investigate two solar cells in more detail. Since both cells were already measured in the previous section the corresponding datapoints in Fig. 2 are marked with a small arrow. The first one is a 15.6×15.6 cm² industrial multicrystalline silicon solar cell while the second solar cell is a 2×2 cm² high-efficiency lab-type solar cell processed at ISFH. Both solar cells have a phosphorous emitter. The emitter sheet resistance of the multicrystalline solar cell is 50 Ω/sq and of the monocrystalline 90 Ω/sq. Note that all values determined for the multicrystalline solar cell correspond to a region of 2×2 cm² in the center.

We obtain the total saturation current densities using the PL ratio approach. The first solar cell shows a J_0 of 4900 fA/cm². In contrast, the second solar cell has a significantly lower value of 430 fA/cm². Note that both values are determined at the corresponding maximum power point.

To separate the contributions of the emitter and the base we apply quantum efficiency analysis to both solar cells. The multicrystalline solar cell yields an effective diffusion length of 110 μm and the monocrystalline of 780 μm.

We determine the base dopant concentration N_A by capacitance voltage measurements and find $N_A = 10^{16} \text{ cm}^{-3}$ (multi-Si) and $N_A = 3.5 \times 10^{16} \text{ cm}^{-3}$ (mono-Si), respectively. With these dopant concentrations we calculate the

base saturation current density to be 3900 fA/cm^2 in case of the multi-Si and 430 fA/cm^2 in case of the mono-Si.

The comparison of these base saturation current densities with the corresponding total J_0 values yields $J_{0e} = 1000 \text{ fA/cm}^2$ in case of the multicrystalline cell and $J_{0e} = 270 \text{ fA/cm}^2$ in case of the monocrystalline cell. The lightly doped and passivated emitter of the monocrystalline solar cell yields a smaller emitter saturation current density and is thus consistent to values published in literature [12]. Note that if other recombination paths like shunts or recombination in the space charge region are present these values can be seen only as upper limits for the emitter saturation current density.

6 OUTLOOK

The benefit of using photoluminescence for the determination of J_0 is a possible spatially resolved application if combining camera-based PL measurements with mappings of the effective diffusion length as for example obtained by spectrally resolved light beam induced current (SR-LBIC) [4].

First investigations regarding spatially resolved PL ratio measurements show that the local analysis carried out for multicrystalline solar cells is more complex. Even though the whole solar cell is at open-circuit conditions this does not necessary hold locally. The emitter and the grid interconnect different grains and resulting balancing currents flow from good into bad grains. Thus, the measured photoluminescence emission under open-circuit conditions is smaller for good grains and higher for bad grains.

7 CONCLUSIONS

We presented an approach to determine the emitter saturation current density of finished silicon solar cells using a combined analysis of photoluminescence and quantum efficiency measurements. We explained the combined approach theoretically and proved experimentally that the ratio of two PL measurements obtained under open circuit and short circuit conditions yields the total saturation current density. For a lab-type solar cell with a passivated lightly doped emitter we obtain $J_{0e} = 270 \text{ fA/cm}^2$ and for a standard industrial solar cell $J_{0e} = 1000 \text{ fA/cm}^2$.

This work was funded by the Federal Ministry for the Environment, Nature Conservation and Nuclear Safety under contract number 0327661.

REFERENCES

- [1] P. Basore, Proceedings of the 23rd Photovoltaic Specialists Conference, Louisville, KY (1993) 147
- [2] D. Hinken, K. Bothe, K. Ramspeck, S. Herlufsen, and R. Brendel, Journal of Applied Physics 105 (2009) 104516
- [3] T. Trupke, R.A. Bardos, M.C. Schubert, and W. Warta, Applied Physics Letters 89 (2006) 044107
- [4] W. Warta, J. Sutter, B. Wagner, and R. Schindler, Proceedings of the 2nd World Conference and Exhibition on Photovoltaic Solar Energy Conversion (1998), 1650
- [5] D. Kane and R. Swanson, Proceedings of the 18th Photovoltaic Specialists Conference (1985), 578
- [6] A. Cuevas, Sol. Energy Mater. Sol. Cells 57, (1999) 277
- [7] D. Clugston and P. Basore, Proceedings of the 26th Photovoltaic Specialists Conference (1997) 207
- [8] J. Metzdorf, Applied Optics 26 (1987) 1701
- [9] B. Fischer, M. Keil, P. Fath, and E. Bucher, Proceedings of the 29th Photovoltaic Specialists Conference (2002), 454
- [10] B. Fischer, Ph.D. thesis, University of Konstanz (2003)
- [11] F. Recart and A. Cuevas, IEEE Transactions on Electron Devices 53 (2006) 442
- [12] M.J. Kerr, J. Schmidt, A. Cuevas and J.H. Bultman, Journal of Applied Physics 89 (2001) 3821